 DOI10.1109/IGARSS46834.2022.9883098

SYNERGISTIC MIXED-LAYER HEIGHT RETRIEVAL METHOD USING MICROWAVE RADIOMETER AND LIDAR CEILOMETER OBSERVATIONS

Araújo da Silva, M. P. [1], Student Member, IEEE,

Rocadenbosch, F. [1,2], Senior Member, IEEE, Tanamachi, R. L. [3], Saeed, U. [4]

[1]CommSensLab-UPC, Department of Signal Theory and Communications (TSC),

Universitat Politècnica de Catalunya (UPC), E-08034 Barcelona, Spain

[2]Institut d'Estudis Espacials de Catalunya (Institute of Space Studies of Catalonia, IEEC),

E-08034 Barcelona, Spain

[3]Department of Earth, Atmospheric, and Planetary Sciences, Purdue University,

West Lafayette, Indiana 47906 U.S.A.

[4]Department of Communications and Networking, Aalto University, Espoo, 00076, Finland.

Correspondence: marcos.silva@upc.edu (M.P.A.S.); roca@tsc.upc.edu (F.R.)

ABSTRACT

This paper tackles synergistic mixed-layer height (MLH) estimation via a combination of microwave radiometer (MWR) and lidar ceilometer (LC)-based estimates. While MLH-MWR estimates rely on potential temperature retrievals, MLH-LC estimates rely on aerosol gradients. The pros and cons of

This research is part of the projects PGC2018-094132-B-I00 and MDM-2016-0600 ("CommSensLab" Excellence Unit) funded by Ministerio de Ciencia e Investigación (MCIN)/ Agencia Estatal de Investigación (AEI)/ 10.13039/501100011033/ FEDER. Data were provided by Jülich Observatory for Cloud Evolution (JOYCE-CF), a core facility funded by Deutsche Forschungsgemeinschaft via grant DFG LO 901/7-1. The work of M.P.A.S was supported under Grant PRE2018-086054 funded by MCIN/AEI/ 10.13039/501100011033 and FSE "El FSE invierte en tu futuro". The European Commission collaborated under projects H2020 ACTRIS-IMP (GA-871115) and H2020 ATMO-ACCESS (GA-101008004).

MLH retrievals obtained from MWR via the parcel method and from LC via an extended Kalman filter (EKF)-based method are used to motivate the synergistic algorithm. The synergistic algorithm is introduced as a maximum-likelihood combination of MLH-MWR and MLH-LC. Two case examples from the 2013 HOPE campaign at Jülich, Germany, are used to show the robustness of the synergistic method and the effect of surface temperature measurement error. Doppler wind lidar retrievals and radiosonde reference MLH estimates are used for validation.

Index Terms— Mixed-layer height, lidar, microwave radiometer, atmospheric boundary layer

1. INTRODUCTION

The atmospheric boundary layer is the most turbulent part of the troposphere, and is directly affected by the earth's surface characteristics. During the day, the warm air near the earth's surface produces vertical plumes (thermals) that create convective circulations, producing the so-called mixed layer (ML). Different kinds of ground-based remote-sensing instruments such as lidar, radar, sodar and microwave radiometer (MWR) are employed to monitor atmospheric parameters, namely, aerosol concentration, temperature, or vertical wind velocity, in which characteristic structures are used as tracers of the ML height (MLH) [1]. Such MLH estimates derived from remote-sensing technologies are often validated using MLH estimates from radiosonde (RS) observations, which are usually taken as the standard reference [2].

The MWR is a passive remote sensing instrument whose spatial resolution becomes coarser with height, thus inserting uncertainty to its measurements. Collaud Coen at al. [1] and de Arruda Moreira et al. [2] have shown successful results when comparing MLH estimations from MWR- and RS-retrieved potential-temperature profiles by applying the parcel method [3] over both. In contrast to the MWR, the lidar ceilometer (LC) is able to retrieve aerosol-backscatter profiles with high and constant spatial resolution (15 or 30 m). The MLH retrieval by means of an extended Kalman filter (EKF) applied to aerosol-backscatter profiles from the LC (hereafter, MLH-LC-EKF) has proven to be an extremely reliable method. Lange et al. [4] showed that, when the BL is convective due to insolation (e.g., in the afternoon), MLH-LC-EKF produced more accurate results than classical MLH retrieval approaches such as the threshold and gradient methods [3]. However, outside the convective regime, the MLH-LC-EKF usually tracked the top of the non-convective residual layer (RL).

In this context, the present work aims to disseminate a synergistic method by [5], combining the

MLH-MWR and MLH-LC-EKF, and illustrate it by means of two case examples. This synergistic method is aimed at combining the best MLH estimates from MWR and LC using a maximum likelihood criterion, in order to provide a more robust MLH estimate at all times of the day. Radiosonde and Doppler wind lidar (DWL)-derived MLH estimates will be used as references.

2. INSTRUMENTS AND METHODS

2.1. Instruments

The measurement data is part of the HD(CP)^2 Observational Prototype Experiment (HOPE) campaign (April 2013 - May 2013) carried out at Jülich ObservatorY for Cloud Evolution (JOYCE) in Forschungszentrum, Jülich, Germany (50°54′31″ N, 6°24′49″ E, 111 m MSL). One of the principal aims of HOPE was to characterize the evolution of the boundary layer over JOYCE for forecasting applications [6]. Relevant JOYCE instruments used here are listed in Table 1.

2.2. Stand-alone MLH retrieval methods

MLH estimation from ceilometer data -. The MLH-LC-EKF estimation method [4] was applied over measurements obtained by the Jenoptik CHM-15k ceilometer 1. The EKF is a time-adaptive method based on Kalman filtering that uses time-successive LC attenuated-backscatter profiles to track the sharp aerosol gradient occurring in the ML-to-free troposphere (FT) transition. As a result, the EKF provided an MLH estimate with the same time resolution as the LC data (15 s).

Estimation from MWR and RS data -. The parcel method (PM) [3] was used to estimate the MLH from both the MWR and the RS. Physical temperature profiles, $T(z)$, retrieved from these instruments were converted into potential temperature profiles, $\theta(z)$. The MLH was estimated as the lowest point in a given temperature profile for which, $\theta(z) > \theta(0)$, where $\theta(0)$ is the surface potential temperature. Because the PM is very sensitive to the surface temperature, we used temperature observations from the JOYCE tower at 2 m as reference. The MLH estimation uncertainty was estimated by perturbing the surface temperature by ± 0.5 K [1].

MLH estimation from DWL data -. First, as a proxy of turbulence, vertical velocity standard deviation (VVSTD) profiles were obtained as described in [7]. Then, the MLH was estimated as the first height at which the VVSTD fell below a predetermined threshold $VVSTD_{th} = 0.4$ m/s [7]. The MLH uncertainty

Table 1: Main specifications of the instruments from the HOPE campaign.

Parameter	Jenoptik CHM-15k ceilometer	Vaisala CT25K ceilometer	DWL (Halo Stream Line XR)	HATPRO MWR[(1)]
Measured parameter [units]	Attenuated backscatter [$m^{-1}sr^{-1}$]		Vertical air velocity [m s^{-1}]	Brightness temperature [ºC]
Sounding range	350-15000 m	60-7500 m	15-10000 m	0-10000 m
Wavelength	1064 mm	905 mm	1500 nm	$6 \sim 5$ mm (V-band)
Raw spatial resolution	15 m	30 m	30 m	50-500 m[(2)]
Raw temporal resolution	15 s	15 s	2 s	$\sim$2.7 min

Notes: [(1)] HATPRO stands for Humidity And Temperature PROfiler. [(2)] 50 m adjacent to the surface, 500 m above 5000 m.

was computed by varying the nominal threshold by 25% (i.e., 0.4 m/s $\pm$ 0.1 m/s) [8]. MLH estimates below 120 m AGL were rejected as unreliable [7].

2.3. MLH synergistic-retrieval method

The synergistic method (hereafter, SYN) combines MLH-MWR and MLH-LC-EKF and their related uncertainties by using Maximum Likelihood (MaxL) weights along with convective daytime information to derive the synergistic MLH estimates. The procedure can be summarised as follows [5]:

(i) The MLH-SYN is computed as the MaxL between MLH-MWR and MLH-LC-EKF when any of

these two conditions hold: (a) their respective uncertainty intervals overlap at least partially, or (b) time t_h falls in the strongly convective interval I = [1000 – 1400] UTC at the JOYCE site. The MLH via MaxL and its uncertainty are computed as

$$MLH_{SYN}(t_h) = \frac{\frac{MLH_X(t_h)}{\sigma_X^2(t_h)} + \frac{MLH_Y(t_h)}{\sigma_Y^2(t_h)}}{1/\sigma_X^2(t_h) + 1/\sigma_Y^2(t_h)}, \tag{1}$$

$$\sigma_{SYN}(t_h) = \sqrt{1/(\sigma_X^2(t_h) + 1\sigma_Y^2(t_h))}, \tag{2}$$

where MLH_i, $i = X, Y$, is the 30-min-average MLH estimate around time t_h and σ_i is the associated uncertainty. Subscripts "X" and "Y" stand for LC-EKF and MWR, respectively. Values σ_i are computed from the covariance outputs of these algorithms [5].

(ii) Out of conditions (i.a) and (i.b) above, we impose the estimated MLH_{SYN} to be the MWR estimate, i.e., $MLH_{SYN}(t_h) = MLH_{MWR}(t_h)$ and, therefore, $\sigma_{SYN}(t_h) = \sigma_{MWR}(t_h)$.

2.4. Bias and bias variability

In the following section, bias and bias variability of the different MLH estimates by the different methods will be compared with reference to the RS in 30-minute intervals. The bias between two instruments, X and $Y = RS$, is computed as

$$bias_{X,RS}(t_h) = MLH_X(t_h) - MLH_{RS}(t_h), \tag{3}$$

and the bias variability as

$$\sigma_{X,RS}(t_h) = \sqrt{\sigma_X(t_h)^2 + \sigma_{RS}(t_h)^2}. \tag{4}$$

3. DISCUSSION OF RESULTS

Figure 1 shows the MLH estimates by each method (Sect. 2.2) for a typical clear day. On one hand, the MLH-MWR coarsely tracked the whole ML daily cycle, from ML development in the morning to its decay in the afternoon, in agreement with the MLH-RS estimates. However, MLH-MWR estimates have much larger uncertainty than MLH-LC-EKF. On the other hand, MLH-LC-EKF estimates were in agreement

with MLH-RS estimates from 0900 to 1500 UTC. Outside of this interval, the MLH-LC-EKF misleadingly followed the residual layer. Notably, from 1200–1500 UTC, MLH-DWL deviates from the other MLH estimates by -500–-1000 m. The cause of this deviation is not known.

From 0800 to 1600 UTC (Figure 1b), MLH-LC-EKF and MLH-MWR estimates had partially overlapping uncertainty bars and, therefore, the MLH-SYN estimates were computed as the MaxL between these two MLH estimates (Sect. 2.3 (i)). Because the MLH-LC-EKF comparatively had much lower uncertainty, it assumed greater weight in the MaxL computation of Eq.(1) and, thus, it became the "tracking reference" for the MLH-SYN method. Outside of this time interval, the MLH-SYN follows the MLH-MWR (Sect. 2.3 (ii)), avoiding the MLH-LC-EKF RL attribution error.

Figure 1c shows the 30-min MLH bias relative to the MLH-RS reference. The MLH-LC-EKF yielded lower bias magnitude than the MLH-MWR at 0900, 1100, and 1500 UTC, but with lower bias variability (1d). At 0700 and 1700 UTC the MLH-SYN followed the MLH-MWR and yielded much lower bias than the MLH-LC-EKF, which became stranded in the RL. From 1000-1400 UTC, the MLH-LC-EKF had a much lower bias variability than all other methods (Figure 1d). Accordingly, one would opt for MLH-LC-EKF over MLH-MWR in spite of the latter's slightly larger bias magnitude. The MLH-DWL bias magnitude was the smallest from 0900-1500 UTC; however, it also had the highest bias variability. (Figure 1d).

The second case example (Figure 2) illustrates a multi-layer scenario and the effects of surface temperature errors on PM-based MLH. Because the PM is critically dependent on the representativeness of the input surface temperature, the bulk Richardson number (bR) method, using RS temperature and wind measurements [3], was used for verification.

Surface temperature errors, as exemplified in Figure 2a from 1000-1700 UTC, manifest in MLH-MWR as MLH estimates with positive bias. An advantage of the SYN algorithm is that these errors do not propagate into the MLH-SYN, because MLH-SYN favors MLH-LC-EKF (which is responsive to aerosol concentration gradients instead of temperature) during most of this time interval.

Correlating 30-min MLH-MWR to MLH-RS_{PM} estimates for convective periods (1000-1400 UTC) during the 31-day HOPE campaign (28 samples) yielded a correlation coefficient of $\rho = 0.67$ when the surface temperature measured by each instrument was the respective PM input. This value increased to $\rho = 0.84$ when using the JOYCE tower temperature.

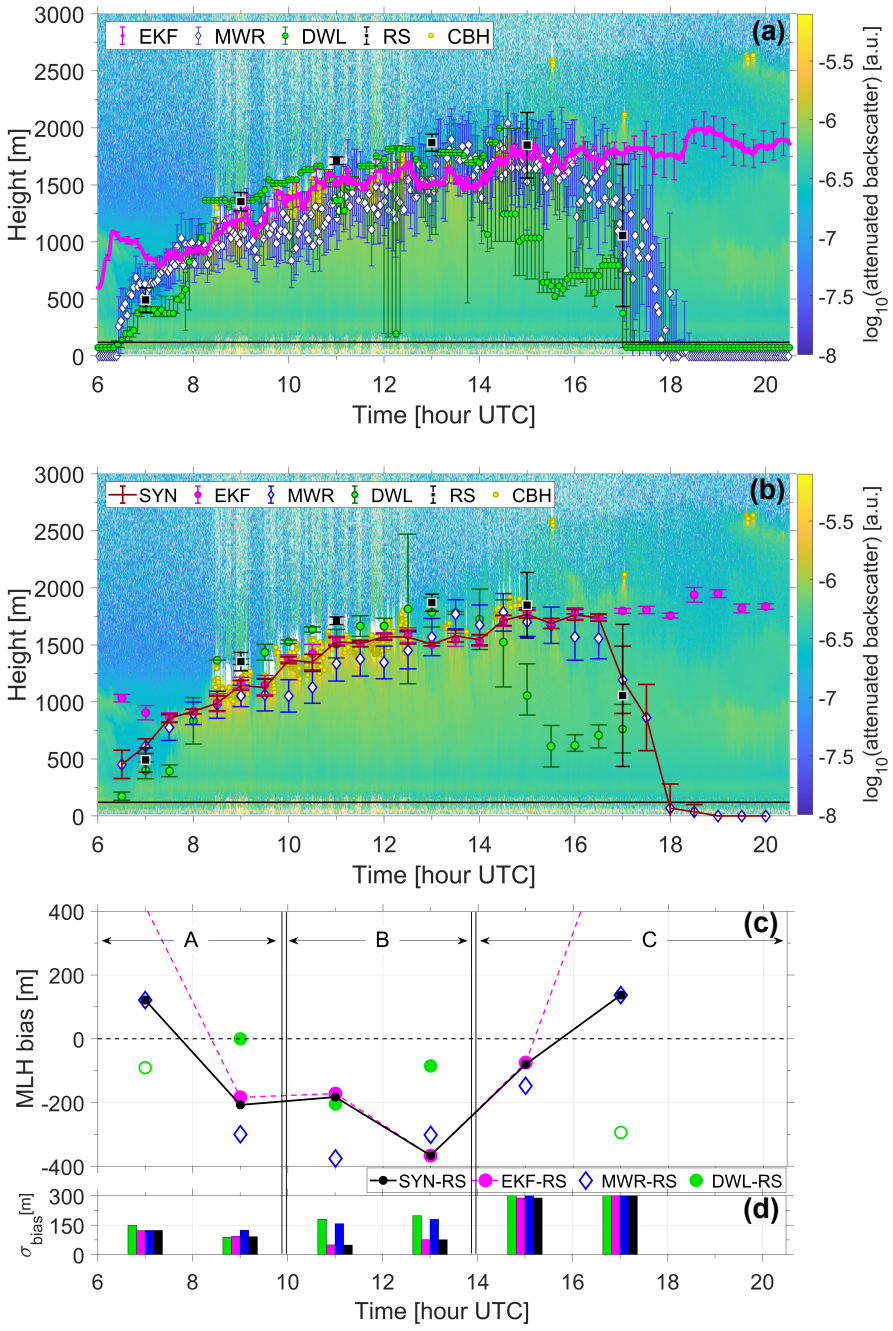

Fig. 1: Case example 05 May 2013, clear day. (a) Color plot of the Jenoptik CHM-15 LC-derived attenuated backscatter. Colored dots: MLH-LC-EKF (pink, EKF label), MLH-MWR (white), MLH-DWL (green), MLH-RS (blue), and estimated cloud base height (CBH; yellow) from the Vaisala CT25K ceilometer. The black-solid line denotes DWL minimum reliable measurement height (120 m). (b) Same as in (a) but resampled to 30-min time resolution [5], and with MLH-SYN (red crosses) added. (c) MLH bias with reference to the RS. (d) Bias variability [5]. Labels (A), (B), and (C) denote the morning-transition, strongly convective, and evening-transition time intervals, respectively.

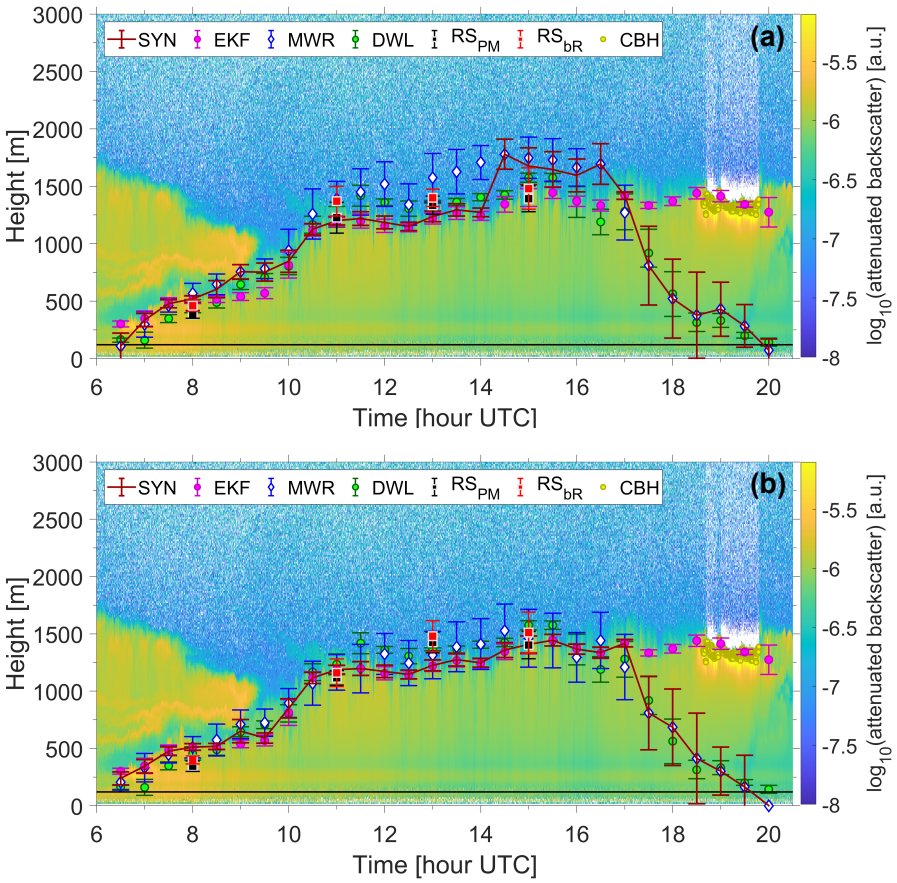

Fig. 2: Case example 04 May 2013. Effects of surface temperature errors on PM-based MLH-MWR. Same format as in Figure 1b. In panel (a), MWR-, RS_{PM}-, and RS_{bR}-MLHs were computed by inputting JOYCE tower surface temperature and, in panel (b), when the surface temperature measured by each instrument was the respective PM or bR input.

4. CONCLUSIONS

A synergistic method for MLH retrieval (SYN) combining MWR and LC-based estimates was presented in the context of previous work [5], along with two case examples from the HOPE campaign [6]. The SYN method used a maximum likelihood algorithm to combine the MLH-MWR and MLH-LC-EKF methods in order to come up with new estimate (MLH-SYN) that overcame the inherent weaknesses of the these two methods in isolation. In isolation, the MLH-MWR suffered from vertical resolution that became coarser with height. Typically, MLH-MWR was greater than that of MLH-LC-EKF, and had an uncertainty given by inherent error in the MWR-retrieved temperature and parcel method surface temperature error. Nevertheless, because a MWR essentially measures radiative emission, and therefore, atmospheric temperature, the

MLH-MWR was able to track the whole ML daily cycle. In contrast, MLH-LC-EKF only tracked the ML top accurately under a strongly convective regime, becoming stranded in the RL after the afternoon-evening transition, when convection died down. MLH-LC relies on atmospheric aerosol gradients (which are not directly dependent on temperature). In summary, our SYN algorithm makes the most of the fine spatial resolution of the MLH-LC-EKF in the convective time interval, and falls back on the MLH-MWR outside of this interval. In this way, MLH can be tracked automatically and reliably, around the clock.

5. REFERENCES

[1] M. Collaud Coen, C. Praz, A. Haefele, D. Ruffieux, P. Kaufmann, and B. Calpini, "Determination and climatology of the planetary boundary layer height above the swiss plateau by in situ and remote sensing measurements as well as by the cosmo-2 model." *Atmos. Chem. Phys.*, vol. 14, no. 23, 2014.

[2] G. de Arruda Moreira, J. L. Guerrero-Rascado, J. A. Bravo-Aranda, J. A. Benavent-Oltra, P. Ortiz-Amezcua, R. Róman, A. E. Bedoya-Velásquez, E. Landulfo, and L. Alados-Arboledas, "Study of the planetary boundary layer by microwave radiometer, elastic lidar and doppler lidar estimations in southern iberian peninsula," *Atmos. Res*, vol. 213, p. 185–195, 2018.

[3] P. Seibert, F. Beyrich, S.-E. Gryning, S. Joffre, A. Rasmussen, and P. Tercier, "Review and intercomparison of operational methods for the determination of the mixing height," *Atmos. Environ.*, vol. 34, pp. 1352–2310, 2000.

[4] D. Lange, J. Tiana-Alsina, U. Saeed, S. Tomás, and F. Rocadenbosch, "Atmospheric-boundary-layer height monitoring using a Kalman filter and backscatter lidar returns," *IEEE Trans. Geosci. Remote Sens.*, vol. 52, no. 8, pp. 4717–4728, 2014.

[5] M. P. Araújo da Silva, F. Rocadenbosch, R. L. Tanamachi, and U. Saeed, "Motivating a synergistic mixing-layer height retrieval method using backscatter lidar returns and microwave-radiometer temperature observations," *IEEE Trans. Geosci. Remote Sens.*, vol. 60, pp. 1–18, 2022.

[6] A. Macke *et al.*, "The HD(CP)^2 Observational Prototype Experiment (HOPE) – an overview," *Atmos. Chem. Phys*, vol. 17, pp. 4887–4914, 2017.

[7] J. H. Schween, A. Hirsikko, U. Löhnert, and S. Crewell, "Mixing-layer height retrieval with ceilometer and doppler lidar: from case studies to long-term assessment," *Atmos. Meas. Tech*, vol. 7, pp. 3685–3704, November 2014.

[8] J. Villalonga, S. L. Beveridge, M. P. A. da Silva, R. L. Tanamachi, F. Rocadenbosch, D. D. Turner, and S. J. Frasier, "Convective boundary-layer height estimation from combined radar and Doppler lidar observations in VORTEX-SE," in *Remote Sensing of Clouds and the Atmosphere XXV*, vol. 11531. SPIE, 2020, pp. 192 – 201.